Article

Neuron

# Functional Networks for Social Communication in the Macaque Monkey

## Graphical Abstract

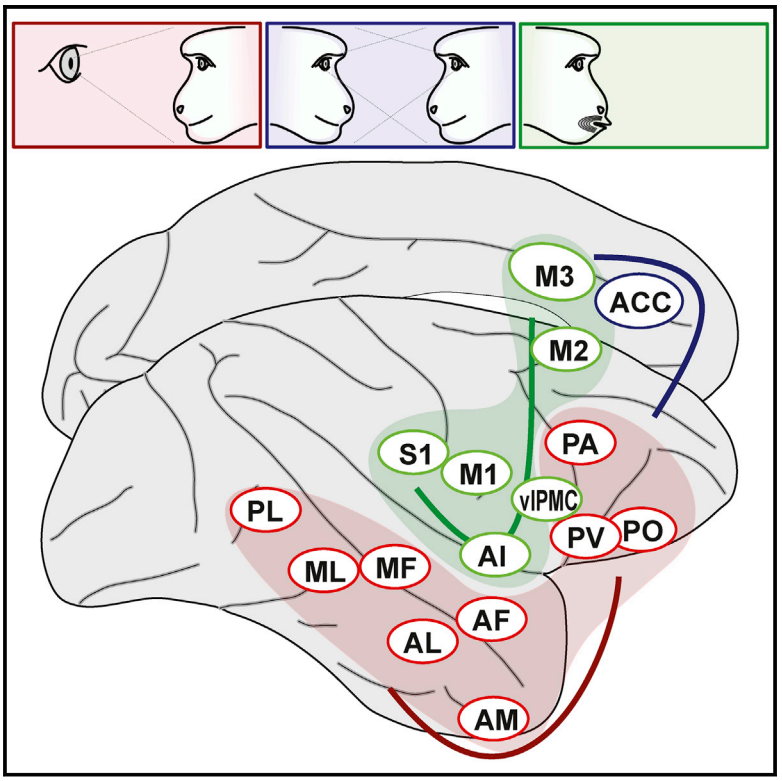


## Authors

Stephen V. Shepherd,
Winrich A. Freiwald

## Correspondence

stephen.v.shepherd@gmail.com (S.V.S.),
wfreiwald@rockefeller.edu (W.A.F.)

## In Brief

Shepherd and Freiwald examine the neural correlates of communication in monkeys during simulated social interaction, discovering networks in the monkey brain for social cognition and social signal production with surprising similarities to those producing human speech.

## Highlights

- Facial perception and facial movement activate non-overlapping networks
- Face-to-face interaction recruits medial prefrontal cortex
- Expression activates medial and ingestion lateral parts of a shared network
- This facial motor network includes homologs of Broca's area

Shepherd & Freiwald, 2018, Neuron *99*, 413–420
July 25, 2018 
https://doi.org/10.1016/j.neuron.2018.06.027

CellPress

Neuron
Article

# Functional Networks for Social Communication in the Macaque Monkey

Stephen V. Shepherd[1,2,*] and Winrich A. Freiwald[1,*]
[1]The Laboratory of Neural Systems, The Rockefeller University, New York, NY 10065, USA
[2]Lead Contact
*Correspondence: stephen.v.shepherd@gmail.com (S.V.S.), wfreiwald@rockefeller.edu (W.A.F.)
https://doi.org/10.1016/j.neuron.2018.06.027

## SUMMARY

**All primates communicate. To dissect the neural circuits of social communication, we used fMRI to map non-human primate brain regions for social perception, second-person (interactive) social cognition, and orofacial movement generation. Face perception, second-person cognition, and face motor networks were largely non-overlapping and acted as distinct functional units rather than an integrated feedforward-processing pipeline. Whereas second-person context selectively engaged a region of medial prefrontal cortex, production of orofacial movements recruited distributed subcortical and cortical areas in medial and lateral frontal and insular cortex. These areas exhibited some specialization, but not dissociation, of function along the mediolateral axis. Production of lipsmack movements recruited areas including putative homologs of Broca's area. These findings provide a new view of the neural architecture for social communication and suggest expressive orofacial movements generated by lateral premotor cortex as a putative evolutionary precursor to human speech.**

## INTRODUCTION

As a rule, animals do not speak. However, all primates communicate, making prominent use of vocalizations and facial expressions. Facial expressions likely derived from evolutionary ritualization of noncommunicative postures indicative of arousal, aggressive or defensive movements, and ingestive actions (Andrew, 1963) and, as Charles Darwin famously noted, reveal otherwise hidden internal emotional states to others (Darwin, 1872). As such, facial expressions form an important category of visual signals in primate societies (van Hooff, 1967). To function as communicative signals, facial expressions must be perceived by a receiver; interpreted; and, at times, answered by a response. Because of their role in communication, facial expressions are more likely to be produced when there is an audience (Fernández-Dols and Crivelli, 2013) and thus depend on the sender's awareness of social context. Despite their importance for emotional processing, communication, and social coordination, little is known about the neural circuits controlling facial expressions and their relationship to circuits of face recognition and social cognition.

Social perception, in the visual domain, relies on face recognition. Face recognition is supported by a network of selectively interconnected temporal and prefrontal face areas with unique functional specializations (Moeller et al., 2008; Tsao et al., 2008a, 2008b; Fisher and Freiwald, 2015; Grimaldi et al., 2016). Although some of the outputs of the system are known, how outputs from this system are used for subsequent behavior remains unknown. In particular, how the face-perception system relays information to facial motor areas during social communication is not understood. An important clue to this question is that facial expression exchange is partly reflexive. For example, humans (Dimberg et al., 2000) and perhaps macaques (Mosher et al., 2011) automatically mimic expressions, much as both primate species automatically follow gaze (Shepherd, 2010). This suggests that dedicated feedforward pathways may link these percepts to their respective reflexive responses. A major output of the face-perception network is the basolateral amygdala (Moeller et al., 2008). The basolateral amygdala is also a major input into anterior cingulate facial motor area M3 (Morecraft et al., 2004, 2007). Area M3, in turn, projects directly to the facial nucleus (Morecraft et al., 2004), which harbors motor neurons directly controlling facial musculature. It is thus a plausible hypothesis that face-perception circuits drive emotional facial expressions in a feedforward circuit from the face-perception areas through the amygdala to the anterior cingulate cortex.

The central role this hypothesis ascribes to area M3 is in line with results from human neuropsychology, which has found a double dissociation between medial and lateral cortical areas in facial motor control. Although lesions to medial frontal cortex impair affective expressions and vocalizations, lesions to lateral frontal cortex impair voluntary gestures and speech (Hopf et al., 1992; Morecraft et al., 2004; cf. Hage and Nieder, 2016). Despite the line of continuity between human and non-human expressions, human language has been argued to lack clear precedent in orofacial communication. Specifically, it has been argued that orofacial communication in non-human primates is too reflexive and simple to constitute precursors of speech and that speech instead must derive from ape innovations in gesture and simulation (e.g., see Arbib, 2005). This reasoning suggests the hypothesis that emotional communications are shared with animals and mediated by medial frontal and subcortical structures, and volitional communication is unique to humans and mediated by lateral (and lateralized) structures (e.g., for vocal behavior; Wheeler and

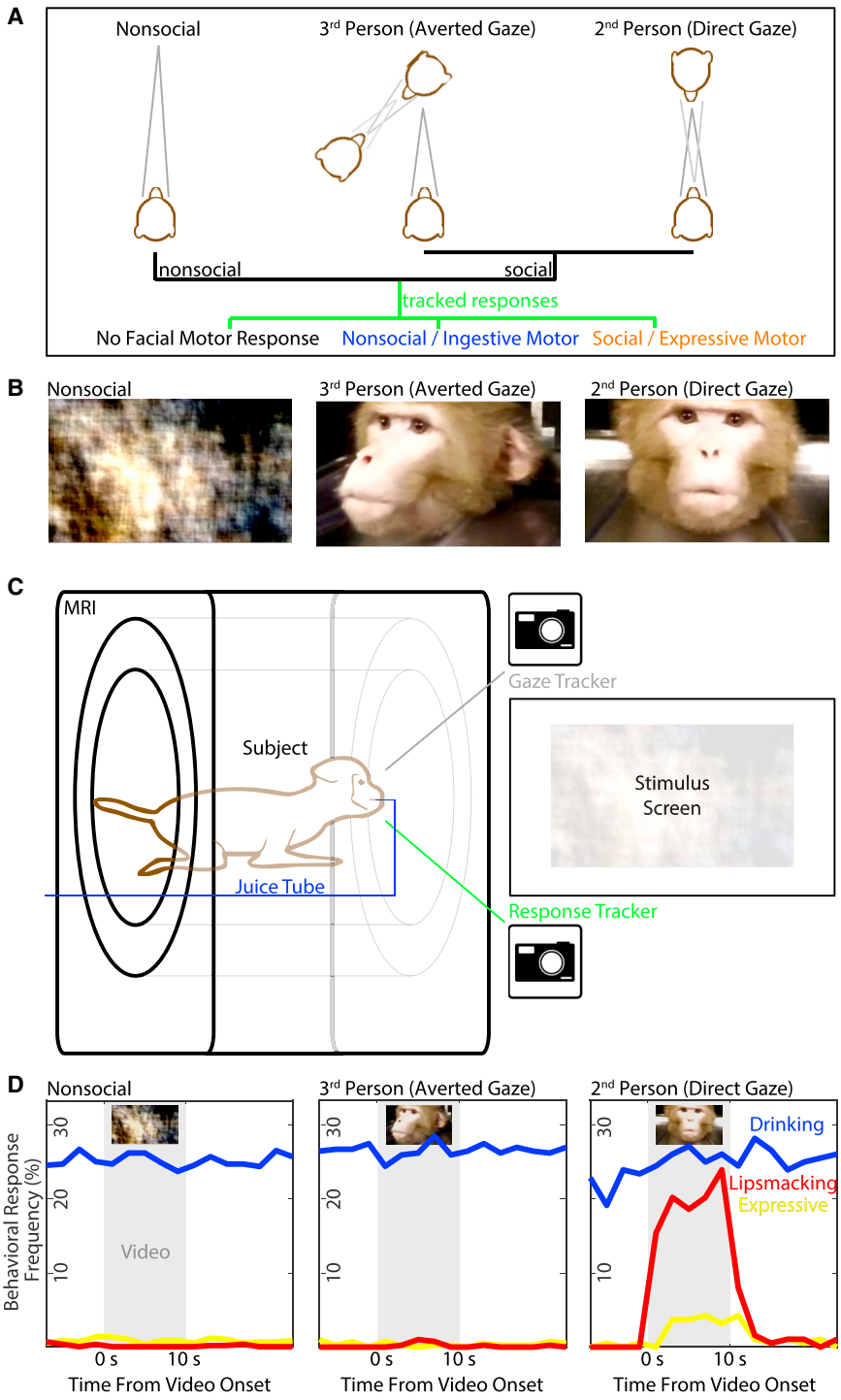


**Figure 1. Simulating Interactions during Monkey fMRI**

(A) Schematic of visual stimuli (top) an observer (middle) might perceive and respond to (bottom). Stimuli can be nonsocial (left) or social directed away (middle) or toward (right) the observer, who might not respond or generate a social or an (unrelated) nonsocial motor response.

(B) Sample frames of three categories of video (left to right: phase-scrambled, socially expressive dynamic faces directed away or toward subject); for stimulus details, see STAR Methods and Figure S1.

(C) Schematic of setup with subject, seated inside the MRI scanner, viewing videos while their gaze and facial movements were recorded by infrared video cameras.

(D) Mean response rates of drinking (blue), lipsmacking (red), and other expressive facial movements (yellow) of ten subjects as a function of stimulus context (left to right) and time relative to the period of video display (light gray). Although drinking behaviors were observed regardless of social context and video presentation, lipsmacks and other expressive behaviors were selectively elicited during second-person video presentation.

Fischer, 2012). However, unlike vocalizations, the neural substrates of primate facial expressions have received almost no attention from neuroscientists—thus, the basic assumption of this hypothesis has not been tested, and the cortical substrates for naturalistic primate communication remain uncertain.

Once produced, facial expressions serve a communicative function only when there is an audience. Interestingly, social context impacts the production of human facial expressions: more are produced when there is an audience (Fernández-Dols and Crivelli, 2013). Communication thus takes place in the so-called second-person context, in which the perceived individual is interacting with the subject. Second-person contexts, it has been argued, elicit fundamentally different cognitive processes than the third-person contexts (the noninteractive observation of others) which have been traditionally used in cognitive science (Mosher et al., 2011; Schilbach et al., 2013; Ballesta and Duhamel, 2015; Dal Monte et al., 2016; Schilbach, 2016). Crucially, it is these understudied second-person contexts for which social communication evolved. Therefore, the study of social communication provides an opportunity to identify the neural circuits of second-person cognition and their relationship to the circuits of social signal production. The minimal instantiating condition for second-person contexts is a sense of mutual perception: we therefore simulated second-person interactions in a controlled "minimal interaction" behavioral framework, testing the hypothesis that these contexts activate circuits specialized for coordinating interactions.

Thus, to understand the neural processing of facial expression production, we need to understand the functional organization of facial motor circuits, their interaction with facial perception

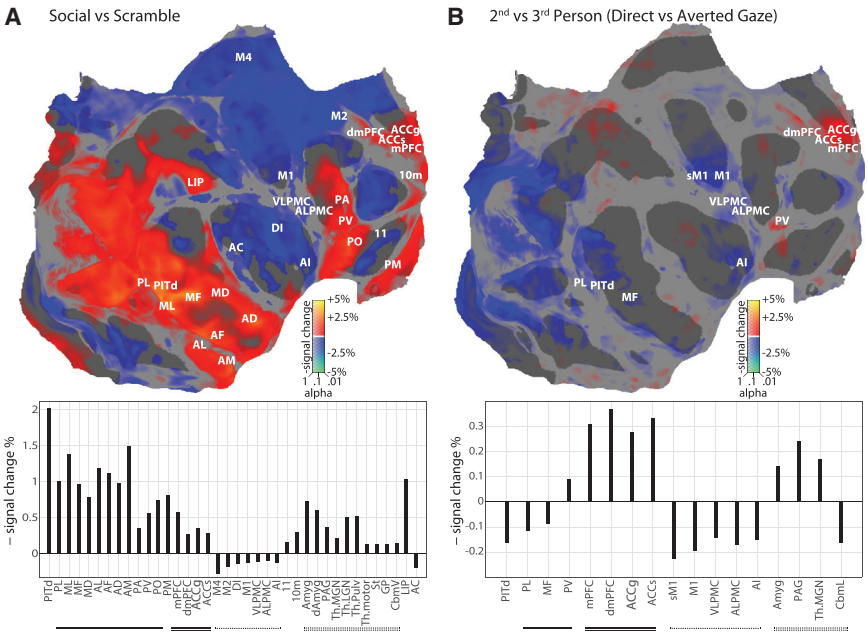


**Figure 2. Neural Responses to Social Stimuli and to Interactive Contexts**

(A) (Top) Digitally flattened map of monkey cortex, in which the occipital pole is toward the left (cut along the calcarine), the temporal pole is at bottom right, the anterior pole is to the right, and the medial wall is in the upper right (cut across the mid-cingulate and posterior to the ascending limb). Areas with increased or decreased activity during social video versus scrambled video are shown in hot or cool colors, respectively, scaled according to percent signal change; significance (corrected for multiple comparisons by estimating the false discovery rate) is indicated by opacity. Note that, in IRON-fMRI, negative signal change corresponds to increased activity. Significantly modulated ROI are labeled. (Bottom) Bar graph of significant ROI responses to social versus scrambled video, including both cortical and subcortical regions, is shown. Upward bars indicate decreased signal and hence increased blood flow and brain activity. Activity changes were calculated by weighted least-squares estimation across all subjects and brain hemispheres (20 hemispheres total); significance was not corrected for multiple comparisons. Face patches are underlined, medial decision associated are doubly underlined, facial motor regions are dash lined, and subcortical regions are double dash lined. Key regions activated by social stimuli include form-selective visual cortex, the temporal and frontal face patch systems, and medial frontal regions.

(B) (Top) Flatmap of increased or decreased activity during second-person social video (direct gaze) versus third-person social video (averted gaze). Significantly affected ROIs are labeled. (Bottom) Bar graph of significant ROI responses to second-person versus third-person video perspectives is shown. Key regions activated by second-person context were largely restricted to medial frontal cortex near the rostralmost anterior cingulate.

circuits, and their sensitivity to second-person context. Using a novel experimental approach, we aimed to address the following questions: What is the functional organization of face motor areas? In particular, are facial expressions generated by medial cortical areas and voluntary face movements by lateral ones? What is the functional relationship between face perception and face motor circuits? Does second-person context facilitate the generation of facial expressions, and how is it represented in the brain?

## RESULTS

### Bringing Social Behavior into the Laboratory

We tackled these questions with two innovations. First, we adapted whole-brain fMRI, which had been so successful unraveling the functional organization of the face-perception network, to the domain of social communication. Second, we developed a paradigm for eliciting social facial movements from macaques within the MR scanner. This allowed us to image neural activity across the brain during social perception, during second- and third-person social information processing, and during social signal production (Figure 1).

The paradigm utilized videos of monkeys' dynamic facial displays taken from three angles (Figures 1B and S1A; see STAR Methods): two from either side of the interaction (generating a third-person perspective) and one from the front, simulating direct eye contact (generating a second-person perspective). Showing the same facial movements from different directions kept all intrinsic properties of the real-world scene identical but changed its social relevance to the subject (Schilbach et al., 2006). As a low-level perceptual control, we also generated videos with systematically phase-scrambled frames, preserving spectral content and motion but destroying shapes. During video presentation, monkeys seated in a scanner (Figure 1C) spontaneously produced affiliative signals, particularly the "lipsmack," whose rhythmic features bear similarities with human speech (Ghazanfar and Takahashi, 2014). These lipsmacks were generated selectively during second-person contexts (Figure 1D). We scored subjects' facial movements within video segments corresponding to each 2-s fMRI frame: out of a total of 16,224 segments, 57% showed no facial movement, 26% drinking, 1% (225) lipsmacks, and 1% nonlipsmack expressions. (The remaining 15% were indeterminately ingestive or communicative or included visible body or hand motion.) Lipsmack versus nonlipsmack responses (see STAR Methods) varied significantly across experimental conditions, with 185 segments of lipsmacking observed during subject-directed social video, 25 in the subsequent blank period, and 15 total across all other conditions ($X^2$[df = 27; N = 13,826] = 2,473; p << 0.001). Thus, second-person context was a nearly obligate prerequisite for the generation of this stereotypic facial movement.

### Brain Responses to Social Stimuli in Social Context

Brain activity was modeled as a function of stimulus condition and parametrically of extraocular facial movement and background body movement as scored by a computer algorithm. Social videos, compared to scrambled controls, activated large parts of cortex (Figure 2A, top; calculation based on brain

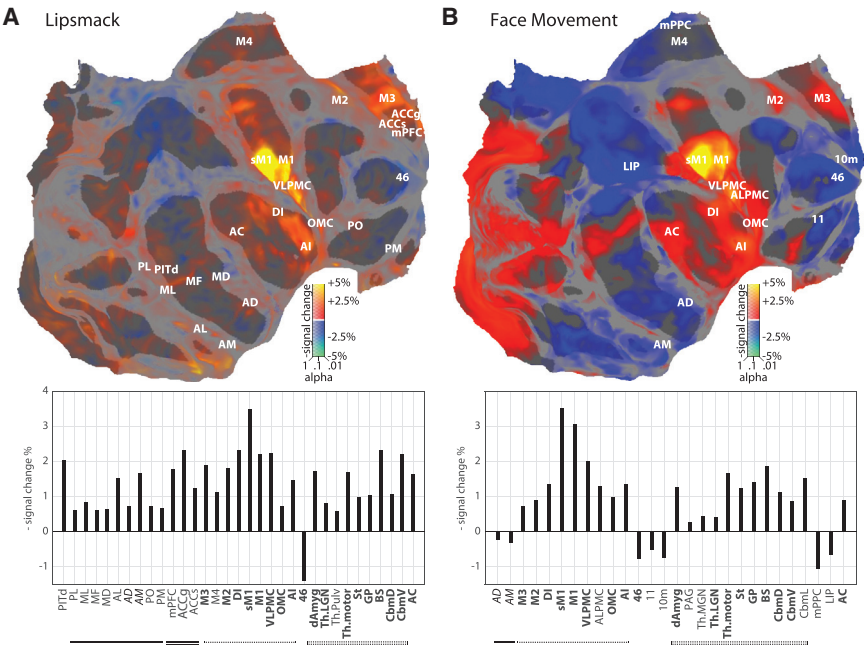


**Figure 3. Neural Responses Associated with Communicative Facial Movement**

(A) (Top) Digitally flattened map of monkey cortex, in which the occipital pole is toward the left (cut along the calcarine), the temporal pole is at bottom right, the anterior pole is to the right, and the medial wall is in the upper right (cut across the mid-cingulate and posterior to the ascending limb). Areas with increased or decreased activity correlated with the presence of subject-produced "lipsmacks" are shown in hot or cool colors, respectively, scaled according to percent signal change; significance (corrected for multiple comparisons by estimating the false discovery rate) is indicated by opacity. Image-based motion estimates have been removed by nuisance regression (see STAR Methods). Significantly modulated ROIs are labeled. (Bottom) Bar graph of significant ROI activity correlated with the presence of subject-produced lipsmacks, including both cortical and subcortical regions, is shown. Upward bars indicate decreased signal and hence increased blood flow and brain activity. Activity changes were calculated by weighted least-squares estimation across all subjects and brain hemispheres (20 hemispheres total); significance was not corrected for multiple comparisons. Face patches are underlined, medial decision associated are doubly underlined, facial motor regions are dash lined, and subcortical regions are double dash lined. Key regions activated include the lateral frontal cortex, supplementary motor cortex, and anterior cingulate motor cortex. Pronounced activity was also recorded in the brainstem facial nuclei, the motor thalamus, and the striatum.

(B) (Top) Flatmap of increased or decreased activity correlated with general computer-scored face movement. Image-based motion estimates have been removed by nuisance regression (see STAR Methods). Significantly affected ROIs are labeled. (Bottom) Bar graph of significant ROI activity correlated with general computer-scored face movement is shown. As in (A), key regions of activation include the lateral frontal cortex, supplementary motor cortex, and anterior cingulate motor cortex, as well as the brainstem facial nuclei, the motor thalamus, and the striatum.

responses to all social video less that to all scrambled video). These activations included visual, temporal, and prefrontal face patches, as expected, as well as medial frontal areas near the rostral cingulate sulcus, areas PITd and LIP (implicated in attentional control and perceived gaze; Shepherd, 2010; Marciniak et al., 2014; Stemmann and Freiwald, 2016), and several thalamic and amygdalar nuclei (Figure 2A, bottom). Activity was reduced in frontal areas 46, 11, and 10 m and large parts of insular, motor, and cingulate cortex. These effects were likely driven by the presence of visual forms and social content. In contrast, when we compared activation between second- and third-person social contexts, activity was much more restricted (Figure 2B; calculation based on brain responses to all direct-gaze unscrambled video less that to all averted-gaze unscrambled video): a medial frontal cluster of areas around the rostral tip of the anterior cingulate cortex (ACC) was significantly more active in second-person context. In fact, the cluster was activated about twice as strongly in second- than in third-person contexts, a pattern rivaled only subcortically, by the periaqueductal gray (PAG). Thus, social context, a prerequisite for social signal production (Figure 1D), appears to be signaled by a spatially confined circuit.

## Brain Activity during the Production of Communicative Social Signals

Facial movements yielded a separate activation pattern (Figures 3A and 3B). Lipsmacks (Figure 3A; calculation based on brain response during manually annotated lipsmacks less that during manually annotated nonmovement, with parametric evaluation of extraocular facial movement ignored) engaged a specific cortical and subcortical motor network, including lateral primary somato-motor cortex (M1 and sM1), ventrolateral premotor cortex (VLPMC), anterior and dorsal insula (AI and DI), an ACC area (M3) just posterior to the second-person context cluster, and subcortical areas, including thalamus, striatum, and brainstem (specifically the facial nucleus, trigeminal motor nucleus, and associated reticular network). A largely identical suite of activations was found for facial movements overall (Figure 3B; calculation based on brain correlates with computer-scored extraocular face movement). Activation in the facial portion of M1 was so strong, it was often detectable during a single facial movement event (Video S1). Thus, in contrast to social perception of second-person contexts, social signal production is supported by a distributed but spatially specific facial motor control system.

In monkeys, the facial movement network exhibited functional specialization, but not dissociation, between communicative and noncommunicative movements. Facial-motor cortex (M1, M2, M3, and VLPMC, but *not* M4; cf. Morecraft et al., 2004) was strongly activated by all facial movements across social stimulus context (Figure 4A, top) and movement type (Figure 4A, bottom). Across all conditions, the lateral motor cortices were most strongly and consistently activated. However, lateral motor cortices were relatively more activated by noncommunicative than communicative facial actions, although the reverse was

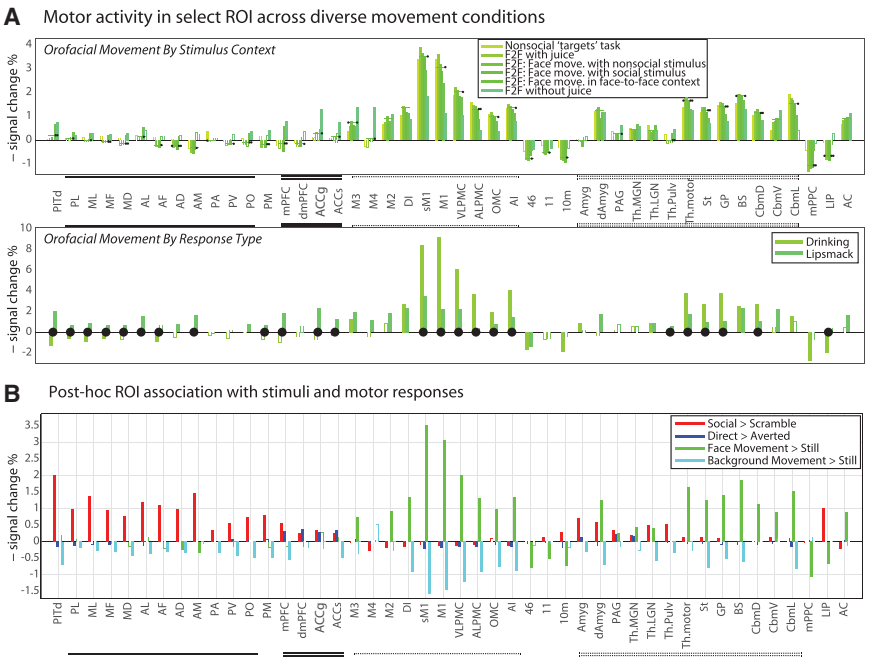


**Figure 4. Functional Selectivity of ROIs to Types of Facial Movement, to Second-Person Context, and to Social Perception**

(A) Neural correlates of produced social versus nonsocial movements were compared in two ways. Above, ROI correlation with computer-scored face movement is plotted under conditions ranging from minimal (left) to maximal (right) sociality; black dots indicated whether the subscore estimates were significantly different from the overall facial movement estimate (i.e., bar plot in Figure 3B; bootstrap $p < 0.05$ where indicated; see STAR Methods). Below, for a subset of subjects (n = 4), neural correlates of experimenter-scored drinking and lipsmack movements are contrasted; black dots indicate significant differences between drinking and lipsmack scores (bootstrap $p < 0.05$ where indicated). These data show that lateral frontal motor and premotor cortex were recruited for both social communicative and nonsocial ingestive movements. Nonetheless, the data show relatively greater recruitment of medial structures during social and of lateral structures during nonsocial movements.

(B) Activity change across all ROIs reflected the presence of dynamic faces (red), "interactive" context (blue), produced facial movement (green), and background movement (cyan); responses are significant *except* where bars are marked with a white line (weighted least square [WLS] across 20 hemispheres; no multiple comparisons correction across areas or conditions). For response reliability across subjects, see Figures S3 and S4.

true for the medial facial-motor regions, including putative area M4 (Figure 4A; see also Figures S3 and S4). Two structures previously implicated in affective signaling, the amygdala and PAG, showed only limited evidence for involvement in lipsmack exchange. Hence, neural control of different facial movements, including expressions, appears to be supported by a single facial-control network with quantitative rather than qualitative division of labor between medial and lateral motor areas.

## The Organization of Brain Circuits for Social Communication

Humans and monkeys tend to match facial expressions, a phenomenon referred to as facial mimicry (Lundqvist and Dimberg, 1995; Mosher et al., 2011). This simple and strong linkage of facial perception to signal production suggests a "vertically" integrated (modular, feedforward) circuit. A candidate pathway with strong anatomical support proceeds from the face-perception system through the amygdala to cingulate area M3 and from there directly to the facial nucleus (Morecraft et al., 2004; Livneh et al., 2012; Gothard, 2014). A potential signature of such a feedforward, vertically integrated module is a gradual transition of selectivity from perception to movement generation. Comparing activation profiles for face perception, social context, and face movement across a large number of regions of interest (ROIs) (Figure 4B), we found ROIs activated by perception but only weakly by context or movement generation; areas activated by context, but not movement; and areas activated by movement with little sensitivity to perception or context. A region dorsal to the amygdala, and more weakly the lateral and medial geniculate nuclei, showed mixed sensitivity to face perception and movement but no sensitivity to context. To capture the distribution of selectivity across ROIs, we performed multidimensional scaling (Figure 5A). The overall pattern of selectivity indicates strong specialization for either of the three functions—face perception, social context, and face movement—but shows little evidence for gradual transitions between them.

A second signature of vertically integrated modules is strong functional connectivity between areas of different specialization within the module. Functional connectivity analysis (Figure 5A) provided little evidence for a strong connection of face perception and movement areas via an amygdala-M3 bridge but instead suggested thalamic and striatal routes. Furthermore, strong functional coupling was found between face perception areas, between cortical and subcortical facial motor areas, and within medial frontal areas. Thus, rather than providing evidence for vertical integration across a social-perception-to-social-response pathway, our functional connectivity analysis suggests the dominance of "horizontal" integration within cortex—that is, within the levels of face perception, of second-person cognition, and of face movement—without strong connections between levels. This view was independently supported by a spatial independent component analysis (ICA) (see STAR Methods). Comparing ICAs across subjects, four large-scale networks were consistently observed (Figure 5B): the first captured activation during social stimulus presentation. The second captured a nonspecific motor network comprising broadly distributed frontal, cingulate, and insular areas, typically suppressed during social stimulus presentation (Figure 1A) and facial movement (Figures 3A and 3B). The third network comprised lateral and medial facial motor areas, M1, sM1, VLPMC, AI, DI, and M3, but not the more anterior social-context-sensitive cluster. The fourth network included this cluster and dorsolateral prefrontal

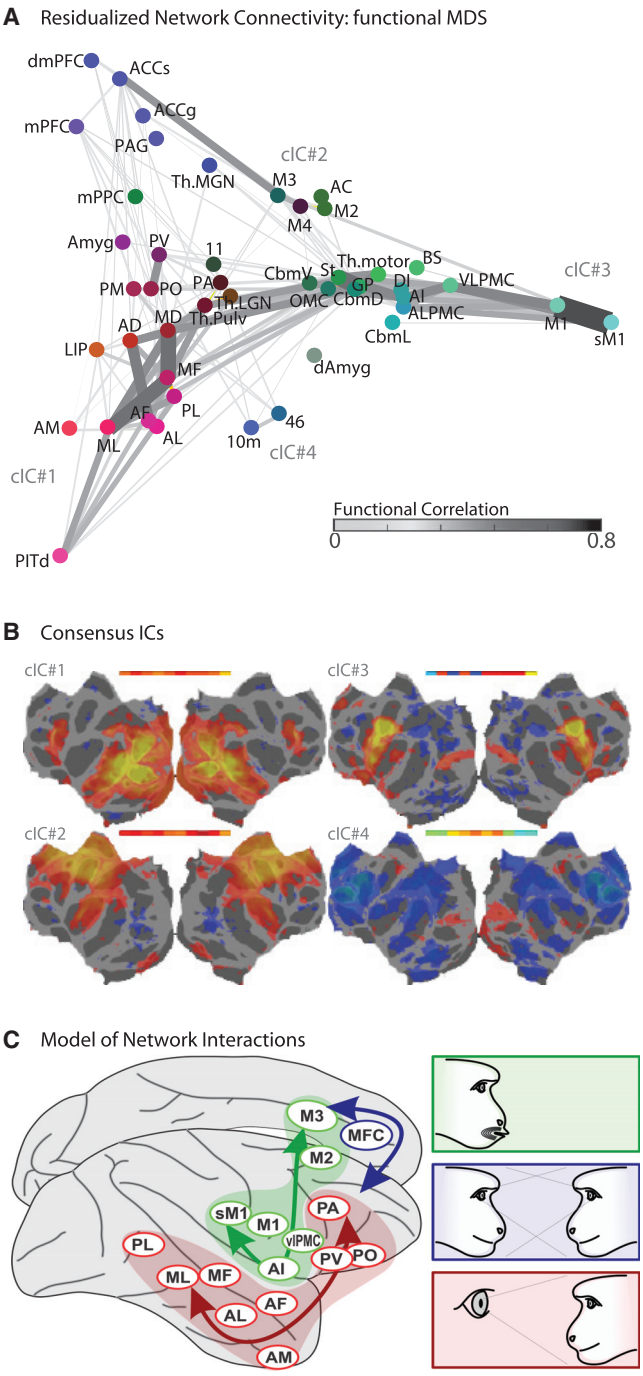


**Figure 5. Network Connectivity during Simulated Social Interaction**

(A) A multidimensional scaling of ROI association with experimental variables (see STAR Methods), linked to illustrate functional connectivity (computed from residuals in these experimental data after accounting for the experimental variables; see STAR Methods). ROI node color indicates relatively stronger sensitivity to social percepts (red), social context (blue), or produced facial movement (green).

(B) In a separate analysis, individual subjects' minimally processed fMRI data were subjected to ICA and common factors were identified across subjects. Networks corresponding to the face patch system (cIC#1) and to a general motor control network (cIC#2) were universally observed, and a face-specific motor control network including the brainstem facial nucleus (cIC#3) and a putative motor inhibition network (cIC#4) were frequently identifiable. The maximal correlation of individual ICs with the common factor is illustrated in inset above the factor map.

(C) Schematic of three independent cortical networks for social communication found in this study: face perception (red); second-person context (blue); and facial expression (green).

areas and may exert executive control. Together, these results suggest multiple functional networks, with at least three functional specializations, engaged during facial communication (Figure 5C).

## DISCUSSION

In this first fMRI study of the neural circuits of social communication in primates, we found a network of cortical and subcortical areas controlling a facial signal, the lipsmack. By systematically monitoring the entire brain, we established which candidate areas—shown by anatomy to project to the facial nucleus (Morecraft et al., 2004), by microstimulation to support vocalization (Jürgens, 2009), or by electrophysiology to contain facial-expression-related cells (Ferrari et al., 2003; Petrides et al., 2005; Coudé et al., 2011; Livneh et al., 2012; Hage and Nieder, 2013; cf. Caruana et al., 2011)—are engaged in routine communication. It is widely held that affective signals are broadly conserved in primates and that more derived, voluntary systems, including speech, are unique to humans (e.g., Arbib, 2005; Wheeler and Fischer, 2012). Moreover, medial and lateral areas of facial motor control are expected to functionally dissociate (e.g., Morecraft et al., 2004; Gothard, 2014; Müri, 2016; cf. Hage and Nieder, 2016). Contrary to these (and our own) expectations, the network supporting the generation of a canonical primate emotional expression—the lipsmack (van Hooff, 1967)—was not centered on medial cortical regions but, in fact, most strongly activated lateral motor and premotor areas with homologies to human speech control.

Yet a medial specialization, relevant for facial expression, does exist: a cluster of areas sensitive to second-person context, including parts of anterior cingulate gyrus, anterior cingulate sulcus, medial prefrontal cortex, and dorsomedial prefrontal cortex. It is centered just anterior to cingulate face motor area M3 and next to areas implicated in high-level social cognition (Schwiedrzik et al., 2015; Sliwa and Freiwald, 2017), revealing a hitherto unknown functional parcellation of macaque medial prefrontal cortex (Yoshida et al., 2011, 2012; Chang et al., 2013; Haroush and Williams, 2015). This cluster may include a homolog to the region activated by second-person contexts in humans (Schilbach et al., 2006).

Face motor areas were distributed, exhibited functional specializations, and were functionally interacting. These are all characteristics the face motor areas share with the face-perception network (e.g., Fisher and Freiwald, 2015; Schwiedrzik et al., 2015). Yet although intra-network interactions were strong, functional interactions between the two networks were limited. Even when face-perception and face-motor areas were near one another, as in the frontal lobe, functional interactions were minimal. Thus, we found little evidence for the hypothesis of a

"vertical" perception-to-production pathway for facial signals. Vertical interactions might transiently occur between networks whose dominant mode of operation is within network.

Given the apparent simplicity of the lipsmack motor pattern (Ghazanfar et al., 2012), activation of an entire multi-area face motor network was surprising. Activation was not restricted to medial facial representations in the anterior cingulate, as predicted for merely affective signals (e.g., Morecraft et al., 2004; Gothard, 2014; Hage and Nieder, 2016; Müri, 2016), but instead prominently included lateral facial representations, associated in humans with voluntary movements, including speech. Importantly, these activations included putative macaque homologs of Broca's area. Prior research has variously identified these homologs as F5 or anteriolateral BA6, BA44, and/or BA45 (Petrides et al., 2005; Neubert et al., 2014). Portions of our motor-associated ventrolateral activations, specifically our anteriolateral premotor cortex (ALPMC) and orbital motor cortex (OMC) ROIs, overlap both F5 and BA44. Our data thus refute the argument that primate facial communication circuits could not have served as a precursor to human speech (e.g., see Arbib, 2005). In fact, lipsmack articulatory patterns are specialized for communication (Shepherd et al., 2012) and their rhythms are reminiscent of human speech syllables (Ghazanfar et al., 2012; Ghazanfar and Takahashi, 2014). We thus show that, like human speech areas, macaque homologs in lateral frontal cortex support communicative articulation. This similarity in cortical function between humans and old-world monkeys suggests that brain networks supporting volitional communication have a common evolutionary origin that arose well prior to the hominin radiation.

## STAR★METHODS

Detailed methods are provided in the online version of this paper and include the following:

- KEY RESOURCES TABLE
- CONTACT FOR REAGENT AND RESOURCE SHARING
- EXPERIMENTAL MODEL AND SUBJECT DETAILS
  - Subjects
- METHOD DETAILS
  - Stimuli
  - fMRI Imaging
  - Imaging Sessions
- QUANTIFICATION AND STATISTICAL ANALYSIS
  - Subject Video Scoring
  - fMRI Analysis
- DATA AND SOFTWARE AVAILABILITY

### SUPPLEMENTAL INFORMATION

Supplemental Information includes four figures, one table, and one video and can be found with this article online at https://doi.org/10.1016/j.neuron.2018.06.027.

### ACKNOWLEDGMENTS

We thank C.A. Dunbar, A.F. Ebihara, M. Fabiszak, C. Fisher, R. Huq, S.M. Landi, S. Sadagopan, C.M. Schwiedrzik, J. Sliwa, and W. Zarco for help with animal training, data collection, and discussion of methods; K. Watson, D. Hildebrand, and S. Serene for comments on the manuscript; L. Diaz, A. Gonzalez, S. Rasmussen, and animal husbandry staff of The Rockefeller University for veterinary and technical care; and L. Yin for administrative support. This work was supported by the Leon Levy Foundation (to S.V.S.), the National Institute of Child Health and Human Development of the NIH (K99 HD077019 to S.V.S.), the National Institute of Mental Health of the NIH (R01 MH105397 to W.A.F.), and the New York Stem Cell Foundation (to W.A.F.). W.A.F. is a New York Stem Cell Foundation-Robertson Investigator. The content is solely the responsibility of the authors and does not necessarily represent the official views of our funders.

### AUTHOR CONTRIBUTIONS

S.V.S. and W.A.F. conceived experiments. S.V.S. performed and analyzed experiments. S.V.S. and W.A.F. wrote the manuscript.

### DECLARATION OF INTERESTS

The authors declare no competing interests.

Received: February 27, 2018
Revised: May 9, 2018
Accepted: June 15, 2018
Published: July 12, 2018

### REFERENCES

Andrew, R.J. (1963). Evolution of facial expression. Science *142*, 1034–1041.

Arbib, M.A. (2005). From monkey-like action recognition to human language: an evolutionary framework for neurolinguistics. Behav. Brain Sci. *28*, 105–124, discussion 125–167.

Ballesta, S., and Duhamel, J.-R. (2015). Rudimentary empathy in macaques' social decision-making. Proc. Natl. Acad. Sci. USA *112*, 15516–15521.

Caruana, F., Jezzini, A., Sbriscia-Fioretti, B., Rizzolatti, G., and Gallese, V. (2011). Emotional and social behaviors elicited by electrical stimulation of the insula in the macaque monkey. Curr. Biol. *21*, 195–199.

Chang, S.W.C., Gariépy, J.-F., and Platt, M.L. (2013). Neuronal reference frames for social decisions in primate frontal cortex. Nat. Neurosci. *16*, 243–250.

Coudé, G., Ferrari, P.F., Rodà, F., Maranesi, M., Borelli, E., Veroni, V., Monti, F., Rozzi, S., and Fogassi, L. (2011). Neurons controlling voluntary vocalization in the macaque ventral premotor cortex. PLoS One *6*, e26822.

Dal Monte, O., Piva, M., Morris, J.A., and Chang, S.W.C. (2016). Live interaction distinctively shapes social gaze dynamics in rhesus macaques. J. Neurophysiol. *116*, 1626–1643.

Darwin, C. (1872). The Expression of the Emotions in Man and Animals (London: John Murray, Albemarle Street).

Dimberg, U., Thunberg, M., and Elmehed, K. (2000). Unconscious facial reactions to emotional facial expressions. Psychol. Sci. *11*, 86–89.

Fernández-Dols, J.-M., and Crivelli, C. (2013). Emotion and expression: naturalistic studies. Emot. Rev. *5*, 24–29.

Ferrari, P.F., Gallese, V., Rizzolatti, G., and Fogassi, L. (2003). Mirror neurons responding to the observation of ingestive and communicative mouth actions in the monkey ventral premotor cortex. Eur. J. Neurosci. *17*, 1703–1714.

Fisher, C., and Freiwald, W.A. (2015). Contrasting specializations for facial motion within the macaque face-processing system. Curr. Biol. *25*, 261–266.

Ghazanfar, A.A., and Takahashi, D.Y. (2014). Facial expressions and the evolution of the speech rhythm. J. Cogn. Neurosci. *26*, 1196–1207.

Ghazanfar, A.A., Takahashi, D.Y., Mathur, N., and Fitch, W.T. (2012). Cineradiography of monkey lip-smacking reveals putative precursors of speech dynamics. Curr. Biol. *22*, 1176–1182.

Gothard, K.M. (2014). The amygdalo-motor pathways and the control of facial expressions. Front. Neurosci. *8*, 43.

Grimaldi, P., Saleem, K.S., and Tsao, D. (2016). Anatomical connections of the functionally defined "face patches" in the macaque monkey. Neuron *90*, 1325–1342.

Hage, S.R., and Nieder, A. (2013). Single neurons in monkey prefrontal cortex encode volitional initiation of vocalizations. Nat. Commun. *4*, 2409.

Hage, S.R., and Nieder, A. (2016). Dual neural network model for the evolution of speech and language. Trends Neurosci. *39*, 813–829.

Haroush, K., and Williams, Z.M. (2015). Neuronal prediction of opponent's behavior during cooperative social interchange in primates. Cell *160*, 1233–1245.

Hopf, H.C., Müller-Forell, W., and Hopf, N.J. (1992). Localization of emotional and volitional facial paresis. Neurology *42*, 1918–1923.

Jürgens, U. (2009). The neural control of vocalization in mammals: a review. J. Voice *23*, 1–10.

Livneh, U., Resnik, J., Shohat, Y., and Paz, R. (2012). Self-monitoring of social facial expressions in the primate amygdala and cingulate cortex. Proc. Natl. Acad. Sci. USA *109*, 18956–18961.

Lundqvist, L.-O., and Dimberg, U. (1995). Facial expressions are contagious. J. Psychophysiol. *9*, 203–211.

Marciniak, K., Atabaki, A., Dicke, P.W., and Thier, P. (2014). Disparate substrates for head gaze following and face perception in the monkey superior temporal sulcus. eLife *3*, e03222.

McLaren, D.G., Kosmatka, K.J., Oakes, T.R., Kroenke, C.D., Kohama, S.G., Matochik, J.A., Ingram, D.K., and Johnson, S.C. (2009). A population-average MRI-based atlas collection of the rhesus macaque. Neuroimage *45*, 52–59.

Moeller, S., Freiwald, W.A., and Tsao, D.Y. (2008). Patches with links: a unified system for processing faces in the macaque temporal lobe. Science *320*, 1355–1359.

Morecraft, R.J., Stilwell-Morecraft, K.S., and Rossing, W.R. (2004). The motor cortex and facial expression: new insights from neuroscience. Neurologist *10*, 235–249.

Morecraft, R.J., McNeal, D.W., Stilwell-Morecraft, K.S., Gedney, M., Ge, J., Schroeder, C.M., and van Hoesen, G.W. (2007). Amygdala interconnections with the cingulate motor cortex in the rhesus monkey. J. Comp. Neurol. *500*, 134–165.

Mosher, C.P., Zimmerman, P.E., and Gothard, K.M. (2011). Videos of conspecifics elicit interactive looking patterns and facial expressions in monkeys. Behav. Neurosci. *125*, 639–652.

Müri, R.M. (2016). Cortical control of facial expression. J. Comp. Neurol. *524*, 1578–1585.

Neubert, F.-X., Mars, R.B., Thomas, A.G., Sallet, J., and Rushworth, M.F.S. (2014). Comparison of human ventral frontal cortex areas for cognitive control and language with areas in monkey frontal cortex. Neuron *81*, 700–713.

Petrides, M., Cadoret, G., and Mackey, S. (2005). Orofacial somatomotor responses in the macaque monkey homologue of Broca's area. Nature *435*, 1235–1238.

Reveley, C., Gruslys, A., Ye, F.Q., Glen, D., Samaha, J., Russ, B.E., Saad, Z., Seth, A., Leopold, D.A., and Saleem, K.S. (2017). Three-dimensional digital template atlas of the macaque brain. Cereb. Cortex 27, 4463–4477.

Schilbach, L. (2016). Towards a second-person neuropsychiatry. Philos. Trans. R. Soc. Lond. B Biol. Sci. *371*, 20150081.

Schilbach, L., Wohlschlaeger, A.M., Kraemer, N.C., Newen, A., Shah, N.J., Fink, G.R., and Vogeley, K. (2006). Being with virtual others: neural correlates of social interaction. Neuropsychologia *44*, 718–730.

Schilbach, L., Timmermans, B., Reddy, V., Costall, A., Bente, G., Schlicht, T., and Vogeley, K. (2013). Toward a second-person neuroscience. Behav. Brain Sci. *36*, 393–414.

Schwiedrzik, C.M., Zarco, W., Everling, S., and Freiwald, W.A. (2015). Face patch resting state networks link face processing to social cognition. PLoS Biol. *13*, e1002245.

Shepherd, S.V. (2010). Following gaze: gaze-following behavior as a window into social cognition. Front. Integr. Neurosci. *4*, 5.

Shepherd, S.V., Lanzilotto, M., and Ghazanfar, A.A. (2012). Facial muscle coordination in monkeys during rhythmic facial expressions and ingestive movements. J. Neurosci. *32*, 6105–6116.

Sliwa, J., and Freiwald, W.A. (2017). A dedicated network for social interaction processing in the primate brain. Science *356*, 745–749.

Stemmann, H., and Freiwald, W.A. (2016). Attentive motion discrimination recruits an area in inferotemporal cortex. J. Neurosci. *36*, 11918–11928.

Tsao, D.Y., Moeller, S., and Freiwald, W.A. (2008a). Comparing face patch systems in macaques and humans. Proc. Natl. Acad. Sci. USA *105*, 19514–19519.

Tsao, D.Y., Schweers, N., Moeller, S., and Freiwald, W.A. (2008b). Patches of face-selective cortex in the macaque frontal lobe. Nat. Neurosci. *11*, 877–879.

van Hooff, J.A.R.A.M. (1967). The facial displays of the catarrhine monkeys and apes. In Primate Ethology. 2006 Edition, D. Morris, ed. (London: Wiedenfeld & Nicolson), pp. 7–68.

Vanduffel, W., Fize, D., Mandeville, J.B., Nelissen, K., Van Hecke, P., Rosen, B.R., Tootell, R.B., and Orban, G.A. (2001). Visual motion processing investigated using contrast agent-enhanced fMRI in awake behaving monkeys. Neuron *32*, 565–577.

Wegener, D., Freiwald, W.A., and Kreiter, A.K. (2004). The influence of sustained selective attention on stimulus selectivity in macaque visual area MT. J. Neurosci. *24*, 6106–6114.

Wheeler, B.C., and Fischer, J. (2012). Functionally referential signals: a promising paradigm whose time has passed. Evol. Anthropol. *21*, 195–205.

Yoshida, K., Saito, N., Iriki, A., and Isoda, M. (2011). Representation of others' action by neurons in monkey medial frontal cortex. Curr. Biol. *21*, 249–253.

Yoshida, K., Saito, N., Iriki, A., and Isoda, M. (2012). Social error monitoring in macaque frontal cortex. Nat. Neurosci. *15*, 1307–1312.

# STAR★METHODS

## KEY RESOURCES TABLE

| REAGENT or RESOURCE | SOURCE | IDENTIFIER |
|---|---|---|
| Chemicals, Peptides, and Recombinant Proteins | | |
| Ferumuxytol (Feraheme) | AMAG Pharmaceutricals | NDC: 59338-775-0 |
| Molday ION | BioPAL | |
| Software and Algorithms | | |
| MATLAB | Mathworks (https://www.mathworks.com) | RRID:SCR_001622 |
| Freesurfer | Freesurfer (http://surfer.nmr.mgh.harvard.edu) | RRID:SCR_001847 |
| JIP | JIP Analysis Toolkit (http://www.nmr.mgh.harvard/~jbm/jip/) | RRID:SCR_009588 |
| MELODIC | FSL (https://fsl.fmrib.ox.ac.uk/fsl/fslwiki/MELODIC) | RRID:SCR_002823 |

## CONTACT FOR REAGENT AND RESOURCE SHARING

Further information and requests for resources and reagents should be directed to and will be fulfilled by the Lead Contact, Stephen V. Shepherd (stephen.v.shepherd@gmail.com).

## EXPERIMENTAL MODEL AND SUBJECT DETAILS

### Subjects

Data was obtained from 10 subadult male rhesus macaques (*Macaca mulatta*), each about 4 years old. All subjects were maternally-reared, transfering to juvenile groups at weaning and into adult colonies at 2 years. The laboratory colony features auditory and visual contact with conspecific males, and study subjects were generally pair-housed. All subjects were fitted with head restraint prostheses using standard lab approaches (Fisher and Freiwald, 2015). Procedures conformed to applicable regulations and to NIH guidelines per the *NIH Guide for Care and Use of Laboratory Animals*. Experiments were performed with the approval of the Institutional Animal Care and Use Committees of The Rockefeller University and Weill Cornell Medical College.

## METHOD DETAILS

### Stimuli

Expressive behaviors were elicited by the first author from 7 stimulus individuals, male rhesus macaques of varying age and familiarity relative to the subjects. Expressions were predominantly lipsmacks, but included other expressions such as silent bared teeth displays, open mouth stares, and mere sustained gaze. Three cameras recorded the stimulus monkeys: two flanking the axis of interaction and one capturing direct 'eye contact' via a half-silvered mirror. Stimulus videos thus appeared to be oriented directly toward (second-person context, or if you prefer, second monkey) or away from (third-person/monkey context) the subject (Schilbach et al., 2006).

We extracted from each of these videos two 10 s video clips in which different social signals were produced in a consistent direction, while expressive content and intensity was allowed to vary. This duration seemed, to human observers, long enough to create a strong sense of communicative intent by the depicted monkey, but short enough that a lack of responsiveness to a viewer could be overlooked. Additional videos were produced by digitally phase-scrambling the originals, using a random constant phase rotation across frames to preserve spatial frequencies and motion content while disrupting visual form. In total, we generated 12 videos each for the 7 stimulus individuals, comprising 3 different perspectives on 2 dynamic sequences of social expression as well as matched, phase-scrambled controls. Stimulus videos were thus were either facing toward the subject (second person), to his left or right (third person, high-order visual control), or were phase-scrambled (nonsocial, low-order visual control). Finally, we stitched videos together so that they appeared sparsely, with ample downtime between presentations and with minimal repeats. Each experimental run consisted of one pseudorandomly selected video from each of the 7 subjects, in pseudorandom order, with 14 s blank periods between each video. The typical recording session consisted of 12 runs with no videos repeated, and would thus include 14 videos of second-person perspectives, 28 of third-person perspectives, and 42 of phase-scrambled controls.

Half of the subjects (S06-10) additionally performed a brief oculomotor task with alternating periods in which they either sustained gaze toward a static visual target or rapidly shifted gaze to look at random targets to garner a fluid reward. Face movements were also recorded in this purely nonsocial task.

Finally, face and body responsive regions were mapped in each subject using variants of a standard localizer task including static images of primate faces, nonprimate objects, and primate bodies (Fisher and Freiwald, 2015).

For details on subjects' participation in experiments, see Table S1.

### fMRI Imaging

Each subject was previously implanted with an MR-compatible headpost (Ultem; General Electric Plastics) using MR-compatible zirconium oxide ceramic screws (Thomas Recording), medical cement (Metabond and Palacos) and standard anesthesia, asepsis, and post-operative treatment procedures (Wegener et al., 2004). Imaging was performed in a 3T Siemens Tim Trio scanner. Anatomical images were constructed by averaging high-resolution volumes gathered under anesthesia (ketamine and isoflurane, 8 mg/kg and 0.5%–2% respectively) in a T1-weighted 3D inversion recovery sequence (Magnetization-Prepared RApid Gradient Echo, or MPRAGE, 0.5mm isometric) with a custom single-channel receive coil. Functional images were gathered using an AC88 gradient insert (quadrupling the scanner's slew rate) and 8-channel receive coil in echoplanar imaging sequences (EPI: TR 2 s, TE 16 ms, 1 $mm^3$ voxels, horizontal slices, 2x GRAPA acceleration). To increase the contrast-to-noise-ratio of functional recordings, we injected monocrystaline iron oxide nanoparticles (feraheme at 8-12 mg/kg for subjects S01-04 or Molday ion at 6-9 mg/kg for subjects S05-10) into the saphenous vein at the beginning of each scan session; in IRON-fMRI, decreases in signal strength correspond to increases in blood flow and hence to neural activity (Vanduffel et al., 2001).

### Imaging Sessions

During each functional imaging session, subjects sat in sphinx position with heads fixed at isocenter. Eye position was measured at 60 Hz using a commercial eye monitoring system (Iscan), and facial movements were captured at 30 Hz using a MR-compatible infrared video camera (MRC). Videos were played in Presentation (Neurobehavioral Systems) stimulus control software. The sparse presentation of social stimuli was designed to maximize the impact of each social interaction while minimizing the subject's exposure to each stimulus (and hence habituation). In some sessions, subjects received juice rewards: either sparsely and randomly or for looking toward the video screen (they were never required to fixate). This helped us to dissociate communicative from noncommunicative facial motion. In other sessions, the juice tube was removed to give an unobstructed view of the subject's mouth and to remove ingestive incentives for orofacial movement (helping us identify naturalistic communicative movements). As described above, half the subjects also participated in an additional nonsocial task during imaging sessions (see Table S1).

## QUANTIFICATION AND STATISTICAL ANALYSIS

### Subject Video Scoring

Facial movements produced by our monkey subjects were recorded in infrared and scored by computer-assisted video analysis, supplemented by targeted manual annotation (Figure S1B). Specifically, the subject's facial behavior in each session was monitored through an MR-compatible camera, which was synched to the stimuli through the placement of a small plastic bicycle mirror behind the subject's head. Subject's facial behavior was extracted through simple computer vision techniques (MATLAB 2015b, custom code) which evaluated local changes in luminance distribution over a manually-defined face-movement window; ovals around each eye were masked from consideration. Additionally, a background-movement window that excluded the face (and the bicycle mirror) attempted to control for body and limb movements; visibility varied across sessions. Finally, the first author and an undergraduate volunteer manually (and blindly, in random order) scored each 2 s period of video as depicting mostly (a) drinking (b) lipsmacking (c) other expressive movements including yawns (d) mixed/miscellaneous/manual movement (e) relative stillness.

### fMRI Analysis

MRI data analysis was performed in FreeSurfer and FS-FAST (http://surfer.nmr.mgh.harvard.edu/) and with custom Linux shell and MATLAB scripts. Raw image volumes were preprocessed through slice-by-slice motion- and slice-time correction (AFNI), aligned to anatomicals and unwarped using JIP Analysis Toolkit (http://www.nmr.mgh.harvard/~jbm/jip/), smoothed (Gaussian kernel, 1mm FWHM), and masked. Data were quadratically detrended in time and analyzed with respect to video stimulus type and facial movement (computer-scored or manually-categorized), generating significance maps by calculating the mean and variance of the response within each voxel to these conditions. GLMs were constructed with binary variables representing stimulus conditions and continuous (computer-scored) variables representing subjects' facial and background movements. Contrasts examined the response to social stimuli (response to social less that to scrambled video), the response to second- versus third-person context (response to direct-gaze less that to averted-gaze video), and the neural correlates of facial movement (indexed by response to the computer-scored continuous variable). To further parse types of motor response, we substituted binary hand-scored variables for the computer-scored continuous variables, contrasting lipsmack and drinking with stillness (responses during lipsmack/drinking less that during stillness). As an alternate means of probing communicative versus noncommunicative movement, we broke apart computer-scored facial responses by context (e.g., computer-scored facial movement during social video, during scrambled video, or during a nonsocial task). Individual subjects' data were registered to the Reveley/McLaren atlases (McLaren et al., 2009; Reveley et al., 2017) and across hemispheres using FSL's FLIRT and FNIRT alignment tools. Regional differences were summarized by averaging unsmoothed voxelwise data, for each subject and at each time point, within each post hoc ROI as defined in common McLaren

space and exported to each subject's individual anatomical space. Data were aggregated across subjects' hemispheres (and ROI, see Figure S2) using weighted least-squares estimation; voxelwise data was FDR-corrected for multiple comparisons. The extent to which ROI signal correlated with facial movement across conditions (Figure 3D) was tested for significance using a bootstrap procedure on WLS differences between the beta value subscores for facial movement within specific contexts versus the beta value for overall computer-scored facial movement (10 subjects) and for the WLS difference between hand-categorized drinking and lipsmack beta values (in 4 subjects: S01-02 and S06-07).

### *Network Analysis*

Spatial ICA was conducted using MELODIC (https://fsl.fmrib.ox.ac.uk/fsl/fslwiki/MELODIC) on the fMRI signal residuals after a blank FS-FAST analysis consisting only of quadratic detrending and the nuisance regression of estimated head motion. Individual ICs were compared across subjects using factor analysis with 'Promax' rotation (MATLAB 2015b) based on the covariance of spatial components in a standardized space, with the most strongly shared factors kept as 'consensus ICs', reconstructed by signed averaging of all spatial components with common-factor loadings greater than 0.5. Functional connectivity analysis was conducted on the fMRI signal residuals of the full FS-FAST analysis, including stimulus video type and autocoded face and background motion parameters as well as motion nuisance regressors. First, correlation coefficients were calculated within each session between each pair of ROI in each hemisphere. Second, we took the median correlation coefficient for each ROI in each hemisphere across runs, tested significance by ttest of the Fischer-transformed correlation values across the 20 hemispheres, and finally used the median correlation value across hemispheres for display. ROI coordinates were illustrated through multidimensional scaling of their signed responses to task conditions, weighting equally the contrasts of social versus scrambled, of second- versus third-person perspective, of background movement, and of facial movement (as aggregated across context- and motion-type subscores). Finally, the color of each ROI was chosen based on the absolute level of modulation of the ROI due to seen faces versus scrambles (red), due to second- versus third-person social perspective (blue), or due to produced facial movement (green), relatively to the maximal observed modulation across recorded ROI for each contrast.

## DATA AND SOFTWARE AVAILABILITY

Further information and requests for software and datasets should be directed to and will be fulfilled by the Lead Contact, Stephen V. Shepherd (stephen.v.shepherd@gmail.com).